

Polymerization of Methacryl and Triethoxysilane Functionalized Stearate Ester: Titanium Dioxide Composite Films and Their Photocatalytic Degradations

Tarik Eren, A. Neren Ökte

Chemistry Department, Bogazici University, 34342 Bebek, Istanbul, Turkey

Received 8 July 2006; accepted 1 February 2007

DOI 10.1002/app.26307

Published online 23 April 2007 in Wiley InterScience (www.interscience.wiley.com).

ABSTRACT: Stearoyl chloride was reacted with 3-(acryloyloxy)-2-hydroxypropyl methacrylate (AHM). Then the resulting product (SAHM) was reacted with 3-amino propyl ethoxysilane (APTES) by Michael addition on the acrylate. The product (SAHMA) is a specialized coupling agent containing an oleophilic 18 carbon alkyl chain, a radically polymerizable methacrylate and an alkoxy silane group capable of coupling to inorganic surfaces, analyzed by FT-IR, NMR, and UV techniques. Photopolymerization and free radical homo and copolymerization of SAHMA with styrene were examined. SAHMA was coupled to powdered titanium dioxide (P25-Degussa) and polymerized. TiO₂ filled materials were analyzed by SEM, UV and TGA techniques. Glass transition temperatures (T_g) of the polymers were determined by differential scanning calorimeter (DSC). Interfacial compatibility between SAHMA

and TiO₂ was demonstrated by FT-IR spectroscopy. The photocatalytic degradation of the TiO₂-SAHMA polymer films was also investigated under medium pressure mercury lamp illumination in air. SAHMA based film containing 2 wt % TiO₂ showed the highest degradation and the highest loss in weight. The weight of the polymer was reduced by 25% of its initial value after irradiation for 40 h. To examine the surface morphology of the irradiated polymer films, SEM analysis was carried out and cavities were detected around TiO₂ particles. The photocatalytic and thermomechanical properties of SAHMA and styrene (STY) based copolymers were also investigated. © 2007 Wiley Periodicals, Inc. *J Appl Polym Sci* 105: 1426–1436, 2007

Key words: titanium dioxide; irradiation; metal-polymer complex

INTRODUCTION

Composites are ideal materials because they exhibit enhanced properties, such as strength, fracture toughness, and impact resistance. These properties depend, in addition to the size of the filler, on the extent of interfacial adhesion between the filler and the matrix and on the level of dispersion of the filler throughout the matrix. To make a successful composite, it is very important to disperse the filler material homogeneously in the matrix and to maximize the interaction between the filler and the matrix.¹ High dispersion can be obtained either by using sol-gel method or by adsorbing effective surfactants, stabilizers, or coupling agents on the filler.^{2,3} Composites, which have inorganic fillers that have some chemical or catalytic activity, are of special interest. Kim et al.³ synthesized TiO₂-poly(methyl methacry-

late) microspheres by *in situ* polymerization of the monomer in the presence of TiO₂ coated with stearic acid. Also, 10 wt % oligomeric dimethyl silicone was added to increase the dispersion stability of TiO₂ in the monomer mixture. Zan et al.⁴ showed the organic modification of TiO₂ surface by using methacryl silane. Yamanaka and coworkers⁵ followed photocatalytic behavior of organografted TiO₂ that was prepared from TiO₂ and *n*-octyltriethoxysilane. The application of miniemulsion polymerization technique to the encapsulation of TiO₂ inside polystyrene latex particles was investigated in detail by El-Aasser and coworkers.⁶ The most successful encapsulation was achieved when TiO₂ particles, either hydrophobic or hydrophilic, were well dispersed in the styrene monomer prior to formation and the polymerization of miniemulsion.

Seed oils have been traditionally used as drying oils and as raw materials for uralkyds and alkyd resins. To form a coating, the unsaturated fatty acids crosslinks through an oxygen initiated auto-oxidation reaction. Metal catalysts, known as driers, can be added to accelerate the drying process.^{7–9} Soucek and coworkers^{10,11} investigated the effects of titanium alkoxide sol-gel precursors on the reaction kinetics of auto-oxidative curing process and compared the

Correspondence to: A. N. Ökte (okteayse@boun.edu.tr).

Contract grant sponsor: DPT; contract grant number: 03K120250.

Contract grant sponsor: B.U. Research Fund; contract grant number: 05B504.

effects of conventional driers. It was reported that incorporation of metal alkoxide in seed oil enhanced the mechanical properties relative to linseed oil coatings. In addition, mixing of metal alkoxides promoted formation of a more homogeneous film without observing microphase separation.^{8,11–14} Kobayashi and coworkers¹⁵ studied composites from renewable resources by using epoxidized plant oils and glycidoxypropyltrimethoxysilane.

The inorganic filler used in this study is a semiconductor, titanium dioxide (TiO₂). Among many semiconductors investigated, TiO₂ is the most commonly used one and Degussa (P-25)-TiO₂ has become a research standard.¹⁶ Its usefulness is known in many applications. The most important application is the photocatalytic oxidation process. This process is known to be a promising technology to degrade a wide range of organic pollutants existing both in the gas and in the liquid phase.^{4–6,16–22} The mechanism of photocatalysis starts with the band-gap illumination of TiO₂ and the production of electron-hole pairs (charge carriers). After separation of these charge-carriers, redox reactions are induced with adsorbed molecules such as molecular oxygen, water, and organic pollutants on the semiconductor surface. Recent studies have already proposed the attractive idea of manufacturing degradable plastics by inclusion of TiO₂ in the composite formulation.^{22–29} For example, photodegradation of polyvinyl chloride accelerated in the presence of TiO₂.^{4,28,29} Solid phase photocatalytic degradation of polystyrene was followed in ambient air under ultraviolet light illumination.^{22,23,27} A higher weight loss rate and a lower average molecular weight were obtained with the inclusion of TiO₂ in the samples. In addition to these, an increase in the carbonyl peak intensity, formation of more volatile organics and higher CO₂ evolution rates were observable when the irradiated samples contained TiO₂.

This study presents a new monomer based on stearic acids that has two functional groups, methacryl and triethoxysilane as shown in Scheme 1. Of these, triethoxysilane groups can bind to TiO₂ and the 18 carbon units alkyl chain form a hydrophobic surface. The methacryl functionality can be photo and thermally polymerized and copolymerized as shown in Scheme 1. The presence of functionalized siloxane on derivatized stearic acid promotes bond formation between inorganic and organic phases. Thus, methacryl and triethoxysilane functionalized stearic acid (SAHMA) behaves as a coupling agent as it contains a radically polymerizable methacrylate, an oleophilic stearate and a triethoxy silane group that is capable of bonding to the TiO₂ surface. The aim of this work is to prepare TiO₂ filled and SAHMA coupled polymers and to observe the effect of the filler on the photodegradation behavior of polymer. The proposed

coupling to the TiO₂ surface is shown in Scheme 2. Coating behavior of stearic acid based films, photo and copolymerization behavior (with styrene) of SAHMA are also followed. SEM, thermal DSC, and TGA techniques are used to examine the disposition of TiO₂ particles. Photocatalytic degradation experiments are performed by using medium pressure mercury lamp under air.

EXPERIMENTAL

Reagents

Stearic acid, 3-(acryloyloxy)-2-hydroxypropyl methacrylate (AHM) and 3-amino propyl ethoxysilane (APTES) were obtained from Aldrich (Milwaukee, WI) and used without further purification. 2,2'-azobis(isobutyronitrile) (AIBN) was obtained from Fluka (Buchs, Switzerland) and was purified by recrystallization from methanol. Commercial TiO₂ from P-25 Degussa (99.5%) with a mean particle size of 21 nm was used. All solvent used were reagent grade.

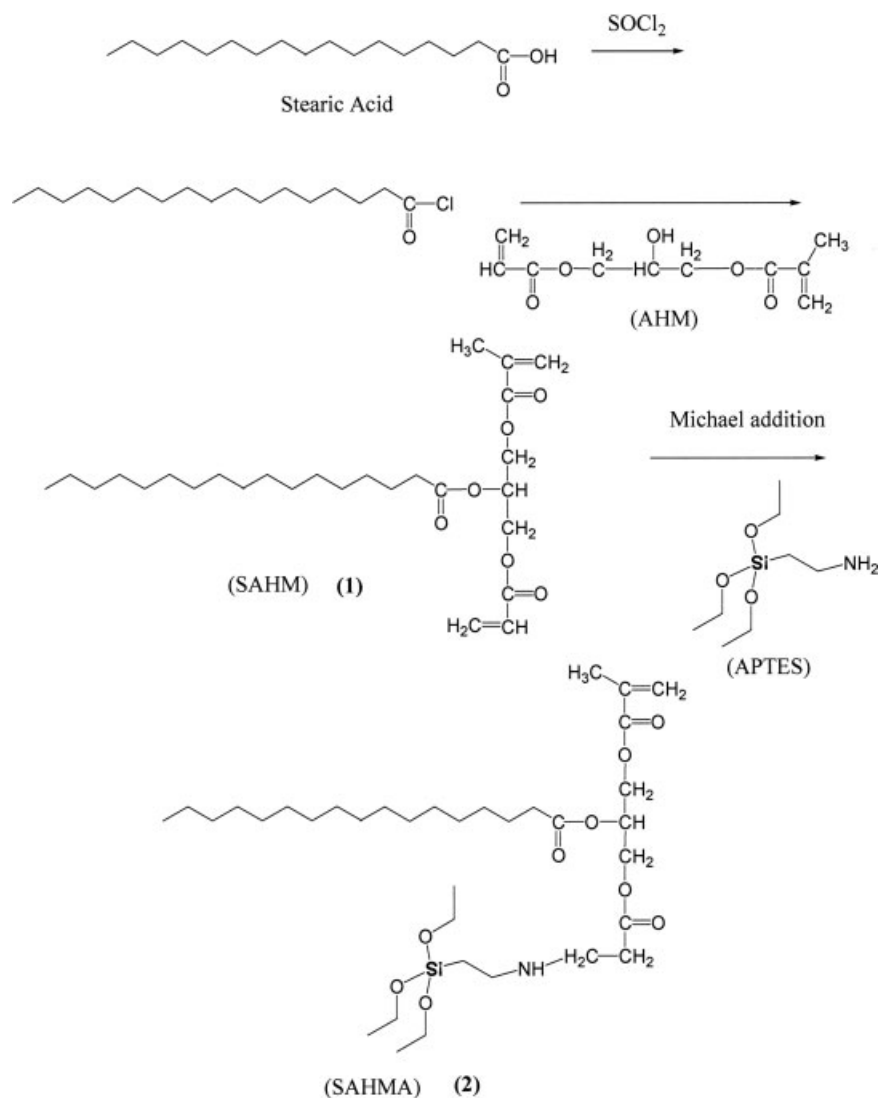
Characterization

¹H and ¹³C-NMR spectra were recorded on Varian 400 MHz NMR (Varian Associates, Palo Alto, CA) using TMS as internal standard operating at 399.986 MHz for proton and 100.587 MHz for carbon. TMS was used as an internal reference and CDCl₃ as an internal lock. The IR analysis was performed on Genesis FT-IR spectrometer (New Castle, DE) using NaCl windows. The glass-transition temperature (*T_g*) for polymers was evaluated using differential scanning calorimetry (DSC). DSC measurements were carried out for the polymers at temperatures from –60 to 150°C using modulated differential scanning calorimetry with a TA Instrument Universal (Giancarlo Scientific, Pittsburg, PA) V2-5H system at a heating rate of 10°C/min under a nitrogen atmosphere. Photopolymerization of SAHMA was done with a TA Instrument Universal (Q 100) with a differential photocalorimeter accessory containing a high-pressure mercury lamp. The surface morphologies of the composite film were observed by scanning electron microscope (SEM, Philips, XL-30, ESEM-FEG). Thermogravimetric studies were performed with a Universal V3.9A TA instruments operating in nitrogen atmosphere. The runs were carried out in dynamic conditions at 10°C/min between 25 and 600°C.

Procedure for the synthesis of SAHMA

Stearoyl chloride

Commercial grade stearic acid 2.25 g (7.9 mmol) and thionyl chloride 5 mL (68 mmol) containing one



Scheme 1 Synthesis of methacryl and alkoxy silane functionalized stearate.

drop of DMF, (*N,N*-dimethylformamide) were mixed at room temperature in 20 mL CH_2Cl_2 . Essentially 100% conversion of acid to acid chloride was obtained, based on the purity of the crude product as determined by ^{13}C NMR spectroscopy (CDCl_3 solution).

^{13}C NMR spectrum showed that acid carbonyl shifts from ($-\text{COOH}$) 178 ppm to ($-\text{COCl}$) 173 ppm.

Reaction of stearoyl chloride with AHM (SAHM) (1)

AHM (2.9 g, 12.7 mmol), stearoyl chloride (2.3 g, 8 mmol), *N,N*-dimethylaminopyridine (DMAP, 0.07 g), and 20 mL tetrahydrofuran (THF) were mixed in a 100 mL round bottom flask and the mixture was stirred at 60°C for 24 h. THF was evaporated under reduced pressure. The product was extracted with 100 mL hexane and the hexane phase was extracted with 3×100 mL aqueous (5%) NaOH and 100 mL H_2O . Hexane phase was dried with Na_2SO_4 and then evaporated under reduced pressure to give

1.56 g (3 mmol, 37% yield) yellow oily product. Product purity was checked by TLC on silica with petroleum ether and ether (7 : 3) as eluent.

IR (KBr): 1636, 808 (m, C=C), 1731 cm^{-1} (s, C=O).

^1H NMR: $\delta = 0.88$ (t, 3H, H-18), 1.10–1.30 (m, 18H, $(\text{CH}_2)_9$), 1.51 (tt, 2H, H-3), 2.20 (t, 2H, H-2), 4.00 (m, 4H, $-\text{HC}(\text{C})-\text{O}-$), 5.00 (br, 1H, $-\text{HCO}(\text{C}=\text{O})\text{CH}=\text{CH}_2$), 5.42 (d, 1H, $-\text{O}(\text{C}=\text{O})\text{C}(\text{CH}_3)=\text{CHaHb}$), 5.71 (d, 1H, $-\text{O}(\text{C}=\text{O})\text{CH}=\text{CHaHb}$), 6.15 (dd, 1H, $-\text{O}(\text{C}=\text{O})\text{CH}=\text{CHaHb}$; $-\text{O}(\text{C}=\text{O})\text{C}(\text{CH}_3)=\text{CHaHb}$), 6.34 (d, 1H, $\text{O}(\text{C}=\text{O})\text{CH}=\text{CHaHb}$).

^{13}C NMR: $\delta = 165, 167$ (C=O), 128, 131 (C=C), 127, 135 ($-\text{CH}_3\text{C}=\text{C}-$), 65, 68 ($-\text{CH}_2\text{O}-$), 22.34–35.37 ($-\text{CH}_2-$), 14.93 ($-\text{CH}_3$).

Synthesis of SAHMA (2)

APTES (0.68 g, 3 mmol) in 3 mL of absolute ethanol was added dropwise to solution of 1.56 g (3 mmol) SAHM in 7 mL of ethanol at 0°C . After the solution

Preparation of SAHMA-TiO₂ films

A 30% THF solution containing SAHMA and 1, 2, or 3 wt % TiO₂ was cast on a slide glass surface (10 cm × 10 cm) and the solvent was evaporated to give films of 40–50 μm thickness. In a typical run, 0.34 g SAHMA, 0.0078 g TiO₂, and 2 wt % AIBN in 5 mL THF were sonicated about 30 min. Polymerization conducted at 60°C for 24 h.

Photodegradation procedure of SAHMA-TiO₂ composite films

The photodegradation performance of SAHMA-TiO₂ composite films was investigated under air at room temperature. The composite films were irradiated by using 250 W medium pressure Hg lamp with an arc size 2 × 4 mm². This lamp contains a number of UV lines of which more than 40% are below 400 nm. Potassium ferrioxalate actinometer was used to determine the number of photons per second and it was found that the lamp emits 1.85 × 10¹⁶ photon/s. A typical size of the film sample was about 5 cm². The light intensity is measured to be 1.48 mW/cm² at 8 cm away from the lamps.^{4,27} The sample was essentially at room temperature during irradiation. UV-vis spectrophotometer (UNICAM) was used to characterize the spectral transmittance of the film before and after irradiation.

RESULTS AND DISCUSSION

Conventional inorganic particles have high surface polarity; therefore, when dispersed in an organic medium, they display low dispersion stability. To increase the stability of dispersion, the interfacial compatibility between inorganic and polymeric materials can be increased by covalently attaching an organosilane-coupling agent. Alkoxysilanes behave as coupling agents between the polymer matrix and the inorganic surfaces that contain hydroxyl groups.^{2,3} In this study, the interfacial compatibility between inorganic and polymeric material is increased by the surface treatment of TiO₂ with methacryl and alkoxysilane functionalized stearate as shown in Scheme 2. TiO₂ filled SAHMA-Styrene copolymer was synthesized by mixing all three components and a free radical initiator and heating the mixture.

NMR analysis

In the first step of the synthesis, stearic acid was converted to its acyl chloride (Scheme 1) and ¹³C NMR spectrum showed that acid carbonyl carbon shifts from 178 to 173 ppm. Stearoyl chloride was then reacted with AHM to give the stearate ester

(SAHM). SAHM was then treated with the aminosilane and the acrylate end underwent a Michael reaction. ¹³C NMR showed that acrylate peaks at 131 and 128 ppm completely disappeared and new carbon peaks were observed at 51.9 ppm (—CH₂—NHCH₂CH₂CH₂(SiOEt)₃) and 51.5 ppm (—CH₂—NHCH₂CH₂CH₂(SiOEt)₃). ¹H NMR spectrum showed that acrylate double bonds at 5.71, 6.15, and 6.34 ppm had disappeared but methacrylate double bonds remained at the same intensity.

FTIR analysis

The chemical structures of SAHMA and SAHMA/TiO₂ composite films (Scheme 2) were characterized by using FTIR spectroscopy (Fig. 1). Figure 1(a) shows the IR spectrum of SAHM. The characteristic methacrylate peaks were observed at 1636 and 808 cm⁻¹. A new ester stretching and ester carbonyl stretching were observed at 1160 and 1731 cm⁻¹, respectively. Hydroxy signal of AHM and carboxylic acid signal of stearic acid were not observed.

Figure 1(b) shows the IR spectrum of SAHMA. The bands at 955 and 793 cm⁻¹ are due to the C—C—O out of phase and in-phase bending. The strong doublets at 1079 and 1103 cm⁻¹ are attributed to symmetric Si—O—CH₂CH₃ stretching. Asymmetric Si—O—CH₂CH₃ stretching coincides with the ester stretching of SAHM at 1165 cm⁻¹. Methacrylate double bond signal was observed at 1637 cm⁻¹. The other methacrylate stretching band at 810 cm⁻¹ coincides with the peak at 793 cm⁻¹ causing a broadening of the band.³¹ Figure 1(c) agrees with the homopolymer of SAHMA in that the methacrylate peaks disappeared after polymerization. Unavoidable hydrolysis and self condensation of silanol group also gives rise to an —OH stretching band at 3300 cm⁻¹ and decreases the intensity of the Si—OCH₂CH₃ stretching band.

The SAHMA-TiO₂ mixture in a THF solution containing 1, 2, or 3 wt % TiO₂ were prepared for polymerization. Before polymerization, when 1 wt % TiO₂-SAHMA mixture is analyzed, a new peak centered at 3300 cm⁻¹ is obtained in addition to SAHMA peaks [Fig. 1(d)]. This peak belongs to the surface hydroxyl (—OH) groups on TiO₂.^{32,33} Introduction of TiO₂ into SAHMA produced a broad and strong absorption band in the range of 400 to 850 cm⁻¹. The intensity of this region increases upon adding higher amounts of TiO₂. IR spectrum of 1 wt % TiO₂-SAHMA polymer is presented in Figure 1(e). After thermal polymerization of the SAHMA in presence of TiO₂, broadening of the 1157 cm⁻¹ peak was observed and a new peak appeared at 1032 and 960 cm⁻¹, presumably due to the Ti—O—Si vibrational stretching.³⁴ Formation of the new Ti—O—Si bond is also evidenced by an increase in the peak

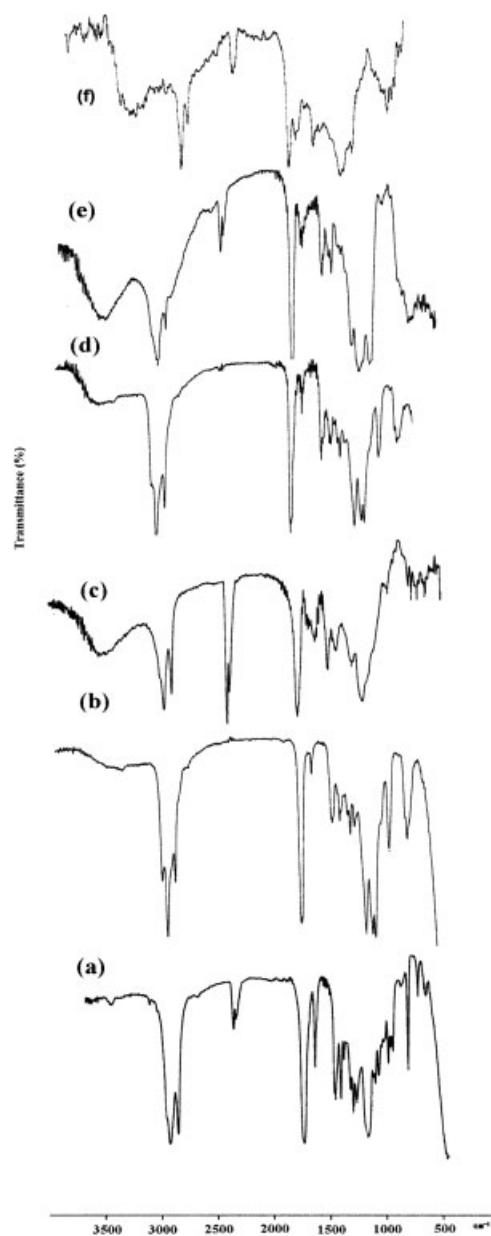


Figure 1 FTIR spectra of (a) SAHM, (b) SAHMA, (c) SAHMA homopolymer, (d) 1 wt % TiO₂-SAHMA before polymerization, (e) 1 wt % TiO₂-SAHMA polymer, (f) 1 wt % TiO₂-SAHMA polymer after irradiation.

intensity at 1165 cm⁻¹. Moreover, disappearance of Si—O—C—C stretching at 955 cm⁻¹ was observed. It was found that the resulting polymer was not soluble in common solvents. This suggested that methacrylate addition polymerization, siloxane-TiO₂ coupling and siloxane self condensation through the silanol groups take place simultaneously. Figure 1(f) shows the photoirradiated sample of 1 wt % TiO₂-SAHMA polymer sample. It was observed that carbonyl peak was broader and ester peak intensity decreased after irradiation. This proves the presence

of TiO₂ in the polymer films that promotes the photocatalytic oxidation of SAHMA.

UV analysis

UV-visible spectra of the films with 2 wt % TiO₂ contents are shown in Figure 2. Pure SAHMA showed one single absorption maximum at 279 nm attributed to the n→π* transition of the carbonyl group [Fig. 2(a)]. The absorption of the SAHMA changed in the presence of the TiO₂ particles especially between 300 and 360 nm. This could be due to the interaction of silane groups and TiO₂ [Fig. 2(b)]. When weight fraction of TiO₂ is increased a broad absorption band is obtained and the band-gap onset of TiO₂ is at about 360 nm. The absorption spectra were not the sum of the absorption spectra of the two components individually, indicating that ground-state charge-transfer or significant electronic interaction occurred between SAHMA and TiO₂ particles. An increase is observed in the absorbance values after thermal polymerization [Fig. 2(c)]. Figure 2(d) shows the degradation of a sample of SAHMA composite containing 2 wt % TiO₂ after irradiation about 40 h. TiO₂ particles dispersed in the films produce photogenerated electrons and holes under illumination. These charge carriers are able to degrade the polymer and form some cavities throughout the film, which cause light scattering. Thus, a low transmittance (high absorbance) was observed.

Photocatalytic degradation of the composite film

TiO₂ is known to be an efficient catalyst for decomposition of a wide variety of materials in both gas

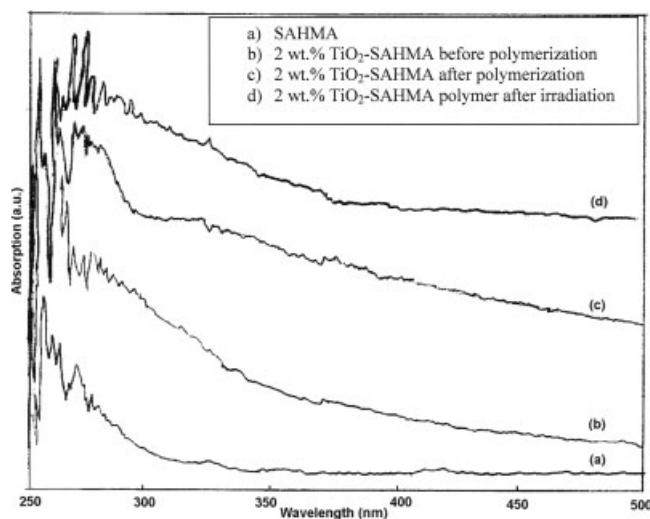


Figure 2 UV-vis absorption spectra of (a) pure SAHMA (b) 2 wt % TiO₂ and SAHMA before polymerization (c) 2 wt % TiO₂ and SAHMA after polymerization (d) 2 wt % TiO₂ and SAHMA polymer after irradiation.

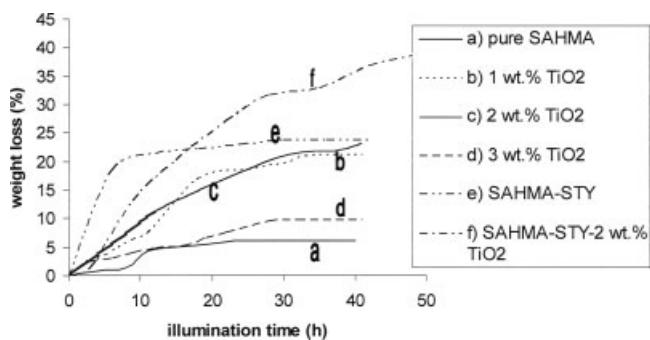


Figure 3 Weight loss of curves of the pure SAHMA (a); SAHMA-TiO₂ based polymer (b–d); SAHMA-STY polymer (e); SAHMA-STY-2 wt % TiO₂ polymer (f); based composite films during irradiation under air.

and liquid phase.^{4,5,16,22} In general, photogenerated holes react with surface hydroxyl groups of TiO₂ to generate surface hydroxyl radicals (TiOH⁺). Likewise, these active species can attack organic molecules, abstract a hydrogen atom, and start a degradation process from the TiO₂ surface. Figure 3 shows the photoinduced weight loss of the polymer films under air. The weight loss rates are much higher for the SAHMA-TiO₂ than the pure SAHMA films and irradiation led to the total reduction of 10–25% in weight. Figure 3 also shows that the weight loss rates of SAHMA-TiO₂ films increased with increasing TiO₂ concentration up to 2 wt %, but decreased at 3 wt % TiO₂ loading. This can be explained by the size of TiO₂ particles. With a higher percentage of TiO₂, particles are aggregated together and reduce the degradation efficiency significantly by (i) decreasing the interface area between polymer and the photocatalytic agent and also (ii) inducing rapid whitening that shortens the light penetration depth into the composite film.⁴ The weight losses of 1 wt % and 2 wt % TiO₂ composite films reached 21 and 25%, respectively, while that of pure SAHMA films reached only 6% loss after 40 h irradiation. Meanwhile, 3 wt % TiO₂ loading caused only 9% weight loss under the same conditions.

Figure 3 also shows the photodegradation weight loss curves of the SAHMA-STY and SAHMA-STY-TiO₂ composite containing 2 wt % TiO₂. Obviously, the weight loss rate of the 2 wt % TiO₂ incorporated film was much higher than that for the unfilled SAHMA-STY copolymer. The weight loss of styrene SAHMA-STY-2 wt % TiO₂ composite film reached 36% while that of pure SAHMA-STY films reached only 20% after 40 h irradiation. It is interesting to note that the weight loss of SAHMA-STY-2 wt % TiO₂ based film was higher than that for SAHMA-TiO₂ based films. This data implies that presence of benzene rings increases photodegradation. Phenyl radicals formed by this process reacts with O₂ and

leads to cleavage of the chain. The detailed mechanistic discussion on photocatalytic degradation of polystyrene-TiO₂ composite film can be found in the literature.⁴

SEM analysis

SEM images of SAHMA homopolymer thin film containing 2 wt% TiO₂ before and after irradiation 40 h are presented in Figure 4. It was observed that TiO₂ particles showed a nonuniform distribution throughout SAHMA films. The average diameter of the particles was found as 20 μm [Fig. 4(A1,A2)].

SEM image of an irradiated sample [Fig. 4(A2)] showed that the degradation of SAHMA started from everywhere on the surface of the films. Degradation between TiO₂ and polymer interface led to the formation of cavities around TiO₂ particles and resulted in a deformed surface. These cavities grow with irradiation time, extending to the inner film and spreading over the film surface simultaneously. Although some of the charge carriers (electrons and holes) are embedded in the film, most of them recombine with each other due to the lack of appropriate trappers inside the film. The surface morphologies of the films showed an obvious difference before and after irradiation. It can be assumed that the photodegradation of SAHMA starts at the catalyst surface and continues to other sites on the films' inner surface. Thus, photocatalytic activity of TiO₂ is proven by SEM analysis of the 2% wt TiO₂-SAHMA composite film and is consistent with the weight loss data shown in Figure 3.

Figure 4(B1,B2) shows the surface morphologies of SAHMA-STY-2 wt % TiO₂ composite films before and after 40 h irradiation. After irradiation of the composite film, big cavities were formed, the film was destroyed and cracks were greatly enhanced. Also, the cavities and the cracks spread over the inner surface and may be produced by the escape of volatile organics from SAHMA-STY polymer.

TGA analysis

Thermal gravimetry (TGA) measurements were carried out for the samples in nitrogen flow with a heating rate of 10°C/min. There are three distinct losses observed during thermal analysis as shown in Figure 5. For example, 2 wt % TiO₂ containing SAHMA homopolymer decomposed with 18% weight loss in the temperature range of 25–200°C. Between 300 and 350°C, a 10% weight loss was observed. There is a sharp weight loss of 29% in the temperature range of 400–500°C. This can be due to the decrosslinking and depolymerization of SAHMA homopolymer. This result also coincides with general methacrylate polymers' ceiling temperatures. At the

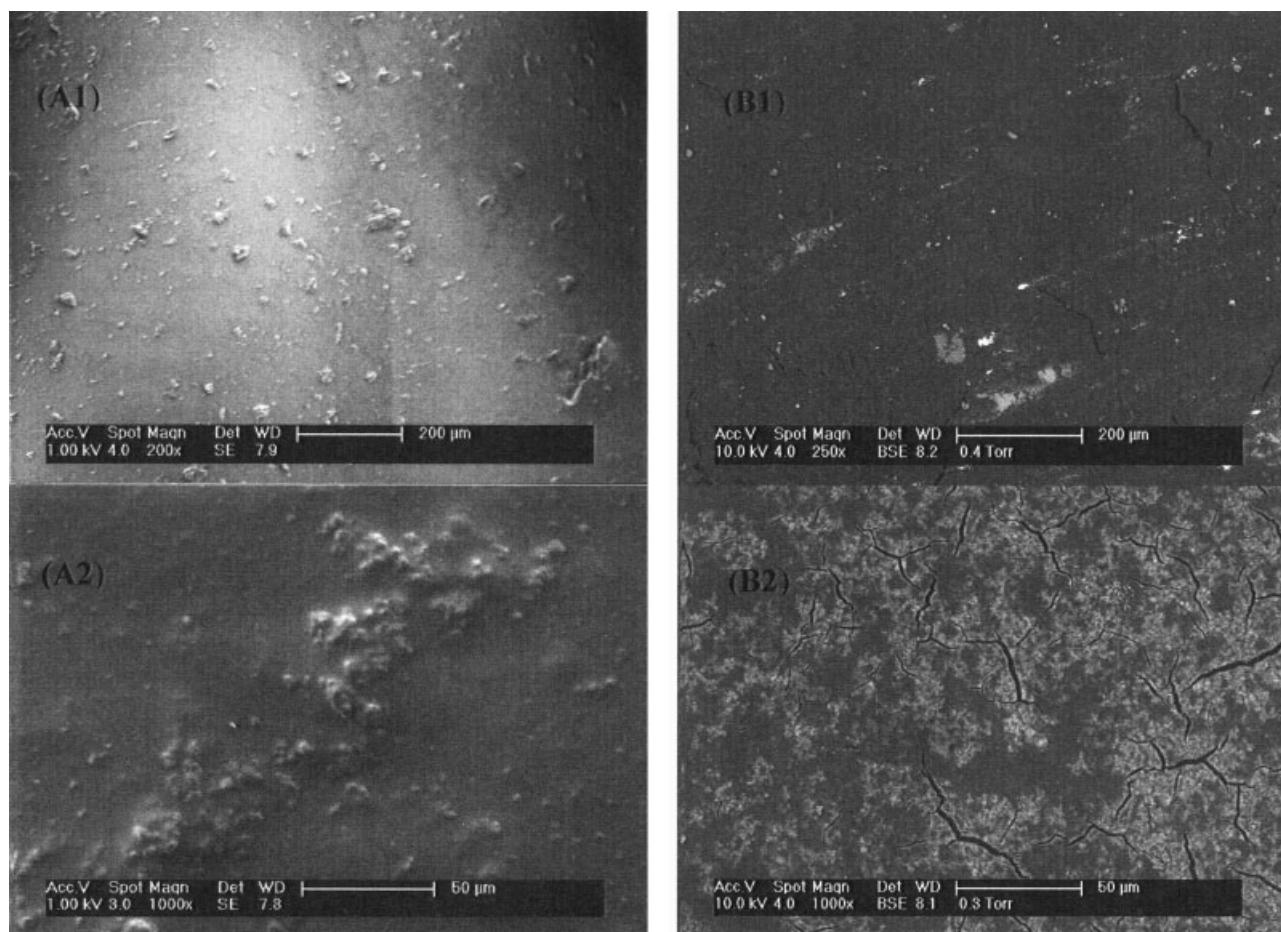


Figure 4 SEM images of (A1) 2 wt % TiO₂-SAHMA based polymer before irradiation (A2) 2 wt % TiO₂-SAHMA based polymer after 40 h irradiation; (B1) 2 wt % TiO₂-SAHMA-STY based polymer before irradiation, (B2) 2 wt % TiO₂-SAHMA-STY based polymer after 40 h irradiation.

end of overall thermal degradation processes, 46, 59, and 62% weight losses were obtained for 3, 2, and 1 wt % TiO₂ samples, respectively. Homopolymer of SAHMA showed 67% weight loss. The TGA data shows that the presence of TiO₂ shifted the weight losses to higher temperatures, indicating that the thermal stability of the composite samples was enhanced. This may be attributed to the restriction in mobility of the polymer chains resulting from: (i) the bonds made by the polymer on the TiO₂ surface via the siloxane groups and (ii) the steric hindrance due to the presence of solid particles.³⁵ Figure 5(e) shows the photodegraded sample of 3 wt % TiO₂-SAHMA polymer. The weight loss of this sample is increased from 46 to 73% as expected. Overall weight loss of SAHMA-STY-2 wt % TiO₂ was 91%, while that of SAHMA-STY copolymer was 96%. In the temperature range of 400–500°C, SAHMA-STY systems exhibited a sharp weight loss from 20 to 92%. This can be due to the decrosslinking of the copolymer and this result is consistent with the general styrene polymers' ceiling temperatures (polystyrene weight lost at 450°C is 100%).^{36,37}

Polymerization of SAHMA

Photopolymerization

The photopolymerization behavior of SAHMA was investigated with photo-DSC. The observed propagation rate (R_p) values and conversion-time plot are given in Figures 6 and 7, respectively. The heat flux as a function of reaction time was monitored using DSC under isothermal conditions, and both the rate of polymerization and conversion were then calculated as a function of time.³⁰ The polymerization rate generally increases with conversion. This is the familiar 'autoacceleration' effect seen in most bulk polymerizations.^{30,38} The conversion-time plot of SAHMA showed a conversion of 92% in 3 min, while SAHMA-STY copolymer reached a conversion of only 20% in the same time period. The reason for such a low conversion and a lower rate of SAHMA-STY system is a gel effect leading to generation of microgels and heterogeneity in the polymer. These affect the limiting translational and segmental mobility of the polymer macroradicals. Photopolymerization of SAHMA showed higher rate and conversion

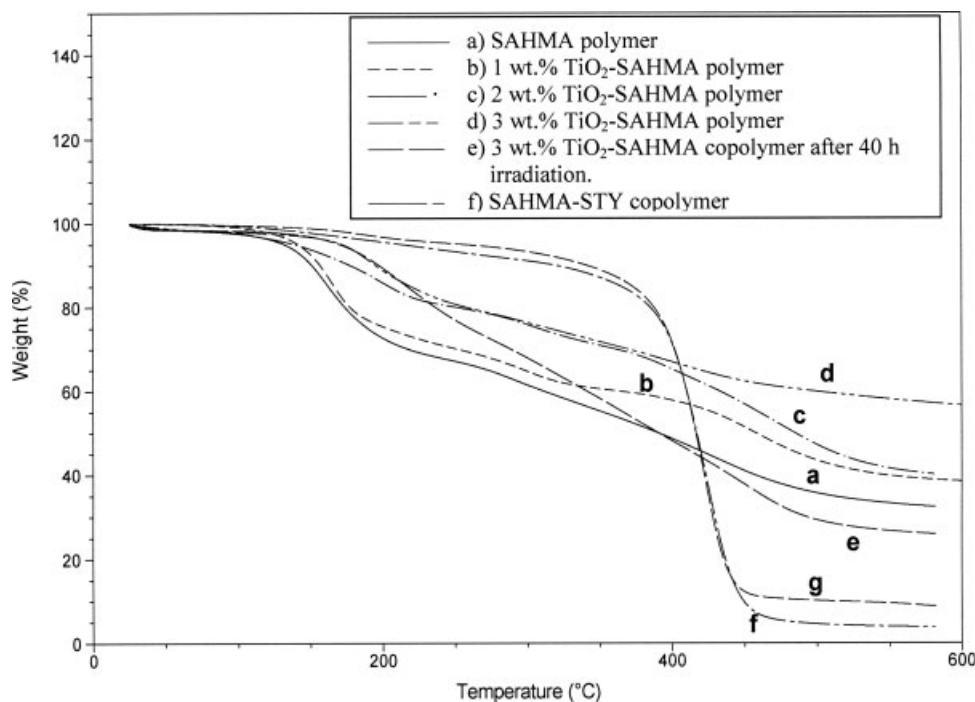


Figure 5 TGA thermogram of (a) SAHMA homopolymer, (b) 1 wt % TiO₂-SAHMA polymer, (c) 2 wt % TiO₂-SAHMA polymer, (d) 3 wt % TiO₂-SAHMA, (e) 3 wt % TiO₂-SAHMA after 40 h irradiation, (f) SAHMA-STY copolymer, (g) SAHMA-STY-2 wt % TiO₂ copolymer.

since its termination rate constant (k_t) is reduced more than its propagation (k_p) rate constant. Thus the overall rate of polymerization and conversion increased.

The reactivities of monomers depend on the polar, resonance, and steric effects of the substituents.³⁹ It is expected that long alkyl groups of SAHMA would decrease the polymerization rate and conversion to some extent however, such decrease was not observed.

Styrene copolymer

Copolymerization behavior of SAHMA was investigated with styrene (STY) in the presence of 2 wt %

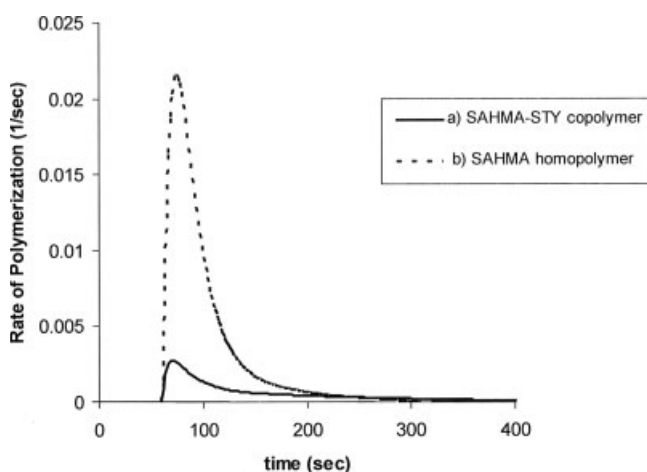


Figure 6 R_p value of (a) SAHMA-STY copolymer and (b) SAHMA homopolymer by photopolymerization.

TiO₂ as well. The polymer was produced in 100% conversion and was not soluble in common solvents. This indicates formation of a crosslinked polymer. Both double bond addition and siloxane self-condensation polymerization took place. SAHMA-STY copolymer without TiO₂ filler was also investigated and the yellow solid polymer was also not soluble in common solvents.

Homopolymer by free radical initiated polymerization

The radical initiated homopolymerization of SAHMA was carried out as neat and in THF solvent in the presence of AIBN. Bulk and solution polymerization resulted in low conversion and produced a cross-linked material, which did not dissolve in common

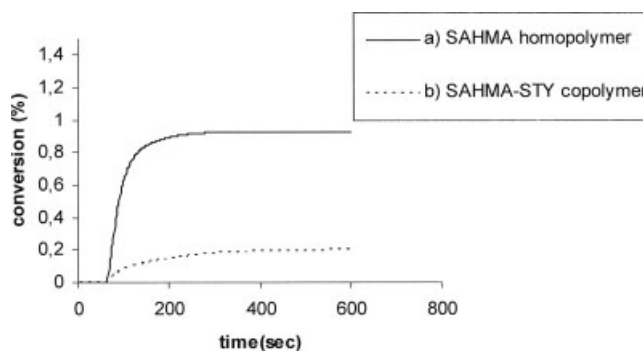


Figure 7 Conversion plot of (a) SAHMA homopolymer and (b) SAHMA-STY copolymer by photopolymerization.

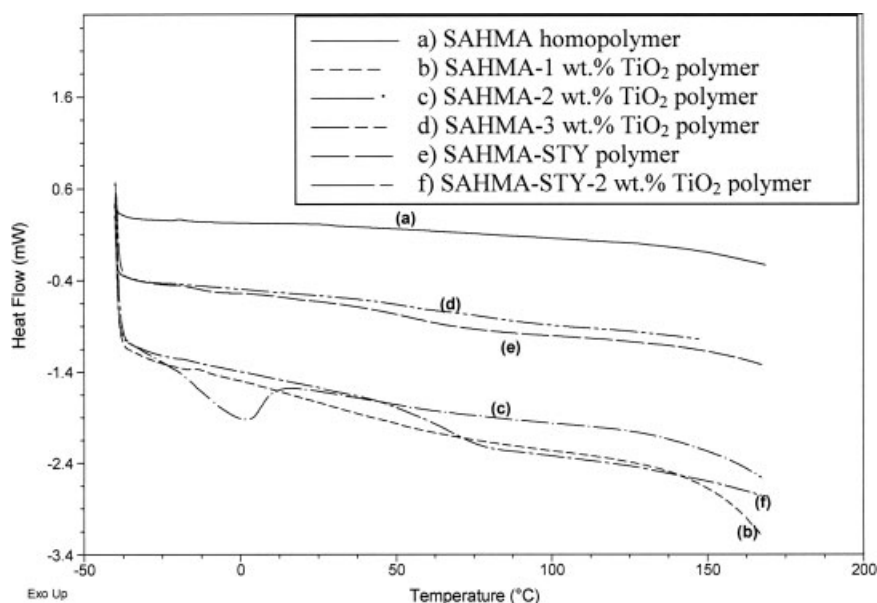


Figure 8 DSC spectra of (a) SAHMA (b) 1 wt % TiO₂-SAHMA (c) 2 wt % TiO₂-SAHMA (d) 3 wt % TiO₂-SAHMA (e) SAHMA-STY (f) SAHMA-STY- 2 wt % TiO₂ polymer.

solvents. The polymer is lightly crosslinked probably due to siloxane self-condensation.

DSC analysis

Incorporation of inorganic materials in a polymer matrix can result in improvement in the thermo-mechanical properties of the polymer. It has been proposed that the motion of polymer chain is restrained due to the presence of TiO₂ particles.³² The restriction in motion is also reflected in a decrease and a broadening of the α -transitions. Meanwhile, with the addition of TiO₂, T_g values increases, attributed to the enhanced crosslinking between the TiO₂ and SAHMA. It is well known that increasing crosslinking density increases the glass transition temperature of the networks. Figure 8 shows the DSC spectrum of the composites. SAHMA homopolymer did not show a characteristic T_g value. 1, 2, and 3 wt % TiO₂ based composites showed a broad transition, which was difficult to assign a T_g value [Fig. 8(b–d)]. For example, the SAHMA-3 wt % TiO₂ based composite showed a broad transition between 50 and 150 °C as shown in Figure 8(d).

SAHMA-STY copolymer showed a broad transition with a T_g value of 45 °C [Fig. 8(e)]. Incorporation of 2 wt % TiO₂ into SAHMA-STY resulted in an increase of the T_g value to 66 °C as expected [Fig. 8(f)].

SUMMARY

- i. Organic–inorganic materials were prepared via polymerization of SAHMA in the presence of TiO₂. FT-IR spectra verified that the SAHMA

had been grafted onto the TiO₂ surface during the polymerization. The Ti–O–Si bonds may be produced through condensation of siloxane groups in the SAHMA with hydroxyl groups on the TiO₂ particles. Photodegradation behavior of SAHMA coating TiO₂ was investigated and it was observed that 2 wt % TiO₂ caused the highest weight loss after 40 h irradiation.

SEM analysis showed the photocatalytic activity of TiO₂ and degradation of SAHMA started from the surface of TiO₂ particles as cavities were formed around TiO₂ particles.

TiO₂ loading (1, 2, and 3 wt %) improved the thermo-mechanical properties of SAHMA homopolymer. DSC spectrum of 3 wt % TiO₂ based composite gave a broad T_g value. According to TGA analysis, 46, 59, and 62% weight losses were obtained for 3%, 2%, and 1 wt % TiO₂ samples, respectively.

Photo and free radical polymerization behavior of SAHMA were also investigated and photo DSC result showed 92% conversion in 3 min. Both polymerization routes resulted in a crosslinked polymer.

- ii. Copolymerization behavior of SAHMA with styrene (STY) was examined. The presence of TiO₂ particles in SAHMA-STY copolymer films greatly promotes the photocatalytic degradation of the composite. Furthermore, thermo-mechanical properties increased in the presence of TiO₂ particles. TGA analysis resulted with overall weight losses of SAHMA-STY and

SAHMA-STY-2 wt % TiO₂ as 92 and 85%, respectively. DSC spectrum of the composites showed that T_g value increased from 45 to 66°C after incorporation of 2 wt % TiO₂ into the SAHMA-STY polymer. Meanwhile, photopolymerization of SAHMA-STY (1 : 1 mol) resulted in 20% conversion.

The SAHMA based polymers may be used as coating materials or adhesives on inorganic and metal surfaces and as toughening additives for thermoplastics. The SAHMA treated TiO₂ composite has a potential to be used as a photodegradable product. Thus, such a process can lead to an eco-friendly disposal of polymer wastes. In addition to these, all the degradation processes can be followed under ambient sunlight irradiation. SAHMA treated TiO₂ surface and polymerization and degradation efficiency with some commercial polymers and reactive diluents with SAHMA are under investigation.

Special appreciation is extended to Prof. Dr. Selim H. Kusefoglu (Bogazici University) for the helpful discussions and the manuscript revision.

References

1. Evora, V. M. F.; Shukla, A. *Mater Sci Eng A* 2003, 361, 358.
2. Tripp, C. P.; Hair, M. L. *Langmuir* 1994, 10, 4031.
3. Kim, J. W.; Shim, J. W.; Bae, J. H.; Han, S. H.; Kim, H. K.; Chang, I. S.; Kang, H. H.; Suh, K. D. *Colloid Polym Sci* 2002, 280, 584.
4. Zan, L.; Tian, L.; Liu, Z.; Peng, Z. *Appl Catal A Gen* 2004, 264, 237.
5. Inumaru, K.; Murashima, M.; Kasahara, T.; Yamanaka, S. *Appl Catal B Environ* 2004, 52, 275.
6. Erdem, B.; Sudol, E. D.; Dimonie, V. L.; El-Aasser, M. S. *J Polym Sci Part A: Polym Chem* 2000, 38, 4441.
7. Wicks, Z. W. Jr.; Jones, F. N.; Pappas, S. P. *Organic Coatings: Science and Technology, Vol. 1: Film Formation, Components, and Appearance*; Wiley: New York, 1992.
8. Sailer, R. A.; Soucek, M. D. *Prog Org Coat* 1998, 33, 36.
9. Sailer, R. A.; Wegner, J. R.; Hurtt, G. J.; Janson, J. E.; Soucek, M. D. *Prog Org Coat* 1998, 33, 117.
10. Ballard, R. L.; Williams, J. P.; Njus, J. M.; Kiland, B. R.; Soucek, M. D. *Eur Polym J* 2001, 37, 381.
11. Wold, C. R.; Soucek, M. D. *J Coat Technol* 1998, 70, 882.
12. Wold, C. R.; Soucek, M. D. *Macromol Chem Phys* 2000, 201, 382.
13. Tuman, S. J.; Soucek, M. D. *J Coat Technol* 1996, 68, 73.
14. Ballard, R. L.; Tuman, S. J.; Fouquette, D. J.; Stegmiller, W.; Soucek, M. D. *Chem Mater* 1999, 11, 726.
15. Tsujimoto, T.; Uyama, H.; Kobayashi, S. *Macromol Rapid Commun* 2003, 24, 711.
16. Prousek, J. *Chem Listy* 1996, 90, 307.
17. Ohko, Y.; Tryk, D. A.; Hashimoto, K.; Fujishima, A. *J Phys Chem B* 1998, 102, 2699.
18. Sadeghi, M.; Liu, W.; Zhang, T. G.; Stavropoulos, P.; Levy, B. *J Phys Chem* 1996, 100, 19466.
19. Sun, L. Z.; Bolton, J. R. *J Phys Chem* 1996, 100, 4127.
20. Choi, W. Y.; Hoffmann, M. R. *Environ Sci Technol* 1997, 31, 89.
21. Caruso, R. A.; Antonietti, M.; Giersig, M.; Hentze, H. P.; Jia, J. *Chem Mater* 2001, 13, 1114.
22. Cho, S.; Choi, W. *J Photochem Photobiol A* 2001, 143, 221.
23. Shang, J.; Chai, M.; Zhu, Y. F. *Environ Sci Technol* 2003, 37, 4494.
24. Ukei, H.; Hirose, T.; Horikawa, S. *Catal Today* 2000, 62, 67.
25. Zhang, Z.; Nishio, S.; Morioka, Y. *Catal Today* 1996, 29, 303.
26. Hirose, T.; Takai, Y.; Azuma, N.; Morioka, Y.; Ueno, A. *J Mater Res* 1998, 13, 77.
27. Shang, J.; Chai, M.; Zhu, Y. *J Solid State Chem* 2003, 174, 104.
28. Robinson, A. J.; Searle, J. R.; Worsley, D. A. *Mater Sci Technol* 2004, 20, 1041.
29. Sivalingam, G.; Madras, G. *Ind Eng Chem Res* 2004, 43, 7716.
30. Nobles, J.; Avci, D.; Mathias, L. J. *Polymer* 2003, 44, 963.
31. Chen, J.; Soucek, M. D. *Eur Polym J* 2003, 39, 505.
32. Zhang, J.; Wang, B. J.; Ju, X.; Liu, T.; Hu, T. D. *Polymer* 2001, 42, 3697.
33. Chiang, P. C.; Whang, W. T. *Polymer* 2003, 44, 2249.
34. Ricchiardi, G.; Damin, A.; Bordiga, S.; Lamberti, C.; Spano, G.; Rivetti, R.; Zecchina, A. *J Am Chem Soc* 2001, 123, 11409.
35. Lerroy, E.; Lopez-Cuesta, J. M.; Ferriol, M.; Cochez, M.; Laachachi, A. *Mater Lett* 2005, 59, 36.
36. Eren, T.; Çolak, S.; Kusefoglu, S. H. *J Appl Polym Sci* 2006, 100, 2947.
37. Brandrup, J.; Immergut, E. H. *Polymer Handbook*, 3rd ed.; Wiley: New York, 1989; Vol. 61.
38. Anseth, K. S.; Kline, L. M.; Walker, T. A.; Anderson, K. J.; Bowman, C. N. *Macromolecules* 1995, 28, 2491.
39. Avci, D.; Kusefoglu, S. H.; Thompson, R. D.; Mathias, L. J. *J Polym Sci Part A: Polym Chem* 1994, 32, 2937.